HHS Public Access

Author manuscript

Biol Psychiatry. Author manuscript; available in PMC 2024 March 15.

Published in final edited form as:

Biol Psychiatry. 2023 March 15; 93(6): 489–501. doi:10.1016/j.biopsych.2022.08.023.

Adaptations in nucleus accumbens neuron subtypes mediate negative affective behaviors in fentanyl abstinence

Megan E. Fox[1,2,*], **Andreas B. Wulff**[3], **Daniela Franco**[2], **Eric Y. Choi**[2], **Cali A. Calarco**[2], **Michel Engeln**[2,6], **Makeda D. Turner**[2], **Ramesh Chandra**[2], **Victoria M. Rhodes**[2], **Scott M. Thompson**[3,5], **Seth A. Ament**[4,5], **Mary Kay Lobo**[2,5,*]

[1.] Department of Anesthesiology, Department of Pharmacology, Penn State College of Medicine, Hershey, PA, USA

[2.] Department of Anatomy & Neurobiology, University of Maryland School of Medicine, Baltimore, MD, USA

[3.] Department of Physiology, University of Maryland School of Medicine, Baltimore, MD, USA

[4.] Institute for Genome Sciences, University of Maryland School of Medicine, Baltimore, MD, USA

[5.] Department of Psychiatry, University of Maryland School of Medicine, Baltimore, MD, USA

[6.] Present address, University of Bordeaux, CNRS, INCIA, UMR 5287, F-33000 Bordeaux, France

Abstract

Background: Opioid discontinuation generates a withdrawal syndrome marked by increased negative affect. Increased symptoms of anxiety and dysphoria during opioid discontinuation are a significant barrier to achieving long-term abstinence in opioid-dependent individuals. While adaptations in the nucleus accumbens are implicated in the opioid abstinence syndrome, the precise neural mechanisms are poorly understood. Additionally, our current knowledge is limited to changes following natural and semi-synthetic opioids, despite recent increases in synthetic opioid use and overdose.

Methods: We used a combination of cell subtype specific viral-labeling and electrophysiology in male and female mice to investigate structural and functional plasticity in nucleus accumbens medium spiny neuron (MSNs) subtypes after fentanyl abstinence. We characterized molecular adaptations after fentanyl abstinence with subtype specific RNAseq and Weighted Gene Co-

[*]To whom correspondence should be addressed: mfox@psu.edu or mklobo@som.umaryland.edu.

Author Contributions

Conceptualization, MEF; Methodology, MEF, SAA, SMT, MKL; Formal Analysis, MEF, ABW, SAA; Investigation, MEF, ABW, DF, EC, CAC, ME, MDT, VMR; Resources, RC, SMT, MKL; Writing-Original Draft, MEF; Writing-Review & Editing, MEF, SMT, SAA, MKL; Visualization, MEF, ABW; Supervision, MEF, SMT, MKL; Funding Acquisition, MEF, SMT, MKL.

Declaration of interests

The authors report no biomedical financial interests or potential conflicts of interest.

expression Network Analysis. We used viral-mediated gene transfer to manipulate the molecular signature of fentanyl abstinence in D1-MSNs.

Results: Here we show fentanyl abstinence increases anxiety-like behavior, decreases social interaction, and engenders MSN subtype-specific plasticity in both sexes. D1, but not D2-MSNs exhibit dendritic atrophy and an increase in excitatory drive. We identified a cluster of co-expressed dendritic morphology genes downregulated selectively in D1-MSNs that are transcriptionally co-regulated by E2F1. E2f1 expression in D1-MSNs protects against loss of dendritic complexity, altered physiology, and negative affect-like behaviors caused by fentanyl abstinence.

Conclusion: Our findings indicate fentanyl abstinence causes unique structural, functional, and molecular changes in nucleus accumbens D1-MSNs that can be targeted to alleviate negative affective symptoms during abstinence.

Keywords

Opioids; nucleus accumbens; abstinence; E2f1; medium spiny neurons; fentanyl

Introduction

Rates of opioid misuse, relapse, and deadly overdose have recently skyrocketed in North America. Drug seizure data indicates that many street drugs and counterfeit opioid pills contain significant levels of the synthetic opioid fentanyl, and that these drugs are often sold to unsuspecting users(1). Highly potent synthetic opioids accounted for 75% of overdose deaths in 2020(2), but remain broadly understudied. Generally, opioid exposure and abstinence engage nuclei within the brain's reward circuitry and cause lasting molecular changes thought to alter circuit function and promote persistent drug use and relapse(3). One hallmark of opioid use is increased negative affect during withdrawal and abstinence(4). Indeed, managing these symptoms is an important component of medication assisted therapies for opioid use disorder, yet our mechanistic understanding of how opioid abstinence changes the brain is primarily derived from studies using natural or semi-synthetic opioids (See 5–7 for recent reviews).

The nucleus accumbens (NAc) is a key locus in brain reward-circuitry that undergoes distinct molecular, cellular, and structural changes during opioid abstinence. Opioid withdrawal reduces dopamine release in the NAc(8–11) and induces numerous transcriptional changes dependent on opioid, sex, and abstinence-duration(12–19). Opioid cessation also causes morphological and electrophysiological changes to NAc neurons. Most studies show decreased dendritic spine density and increased excitatory drive, however the physiologic responses are heterogenous, often NAc subregion specific, and in some cases there are no changes or a decrease in excitability dependent on the paradigm(20–32).

The NAc, located in the ventral striatum, contains primarily medium sized GABAergic spiny projection neurons that are divided into two subtypes based on dopamine receptor expression. *Drd1* or *Drd2* expressing neurons (D1- and D2-MSNs, respectively) have little overlap in their projection targets(33–35), and often have opposing roles in driving drug-

and reward-related behaviors(36–43). Increased activity in D1-MSNs is typically considered "pro-reward" and D2-MSNs "anti-reward," but there is an increasing number of exceptions in different parts of the striatum(44–51). Much less is known about specific MSN-subtypes in opioid abstinence(17,20,21,23,25), especially synthetic opioid abstinence, and females were often excluded from previous studies. Further, many studies single-house animals, an added stressor that impacts drug-related behavior(52–55).

Based on our previous work showing NAc D1-MSNs drive negative affect-like behavior after chronic stress(56–58), we hypothesized D1-MSNs play a key role in increased negative-affective behaviors in synthetic opioid abstinence. We use numerous neuron subtype-specific techniques to show fentanyl abstinence causes dendritic atrophy, increased excitatory drive, and molecular changes specific to NAc D1-MSNs in both sexes. We further show that negative-affective behaviors and NAc D1-MSN morphologic and physiologic changes can be prevented by targeting the transcriptional regulator E2f1.

Methods and Materials

Experimental Subjects

All experiments were performed in accordance with the Institutional Animal Care and Use Committee guidelines at University of Maryland School of Medicine (UMSOM). Gonadally male and female mice on a C57/Bl6 background were given food and water *ad libitum*, bred and housed in UMSOM animal facilities on a 12:12h light:dark cycle. Male CD-1 retired breeders (Charles River,>4 months) were used as aggressors for SDS. Mice were 8–10 weeks old during experiments and randomly assigned to groups. Behavioral experiments were conducted in separate cohorts to (1) keep the abstinence time point consistent between all experimental measurements throughout the study,(2) minimize the influence of repeated handling on anxiety-like behavior(59), (3) and to avoid potential changes to translating mRNA induced by behavioral testing.

All procedures are detailed in Supplemental Information.

Statistics—Mice with off-target virus injection sites were excluded. All statistical tests were performed in GraphPad Prism 9 and JASP accounting for sex as a biological variable. Due to the limited number of significant sex effects or sex interactions (α=0.05), sexes were combined except where noted. Prior to post-hoc comparisons, we ensured data normality and sphericity with built-in GraphPad/JASP functions. To account for multiple cells from the same animal, we used nested t-tests. We used mixed-effects analysis to analyze number of action potentials per current injection due to one missing value. For Nanostring and RNAscope, we used unpaired t-test independently in each cell-type. A detailed statistics table, including sex effects and any variance corrections is in Supplemental File 1. Sample sizes were determined based on prior literature and with the goal of reducing unnecessary repetitive experiments.

Results

Homecage fentanyl abstinence is associated with increased negative affective behavior and reduced D1-MSN dendritic complexity

Here we designed a fentanyl exposure and abstinence paradigm that allowed for intermittent drug delivery, minimized experimenter handling, and prevented social-isolation. We first established our paradigm was sufficient to increase negative-affect-like behaviors associated with opioid abstinence (Fig1A. Sexes combined due to no sex effects; Supplemental File 1). We found fentanyl-abstinent mice had reduced social-interaction time in a 3-chamber social interaction test (Fig1B,p=0.047) and decreased open arm time in the elevated plus maze (Fig1C,p=0.019). To assess if the fentanyl paradigm was sufficient to generate physical dependence, we administered 1 mg/kg naloxone and observed precipitated withdrawal signs in both sexes. We found increased global withdrawal scores in fentanyl-naloxone mice relative to water-naloxone (Fig1D,p=0.002). Since opioid dependent individuals can exhibit an exacerbated stress response(61), we also tested male mice for susceptibility to a 1-day social defeat stress(Fig1E). We found decreased interaction time (increased susceptibility) in fentanyl-abstinent mice subject to subthreshold stress(Fig1F,p=0.0017, Sidak's after 2-way ANOVA; drinking in FigS1A).

We next asked how fentanyl abstinence altered dendritic morphology of medium spiny neuron (MSN) subtypes in the nucleus accumbens core (NAc). We used a low-titer Cre-dependent virus to sparsely label MSN subtypes in D1- and A2A-Cre mice (56) (Fig1G–H; drinking in FigS1B). We found fentanyl abstinence decreased D1-MSN dendritic complexity as measured by reduced Sholl intersections (Fig1I,p<0.05, 40–70 μm from soma, Sidak's after 2-way ANOVA), branch points (Fig1J,p=0.005, nested t-test), and total dendritic lengths (Fig 1J,p=0.003, nested t-test). D2-MSN dendritic complexity was unaltered by fentanyl abstinence as measured by equivalent Sholl intersections(Fig1K), dendritic lengths(Fig1L), and branch points(Fig1L, p's>0.05). There were no robust effects on dendritic spine density in either MSN subtype (FigS1C, p's>0.05).

To ensure changes to MSN morphology resulted from fentanyl abstinence and not fentanyl alone, we performed similar experiments in mice that did not undergo abstinence. These mice were perfused at a timepoint where bottles would normally be replaced with water. We examined dendritic complexity in fentanyl-exposed, but not abstinent mice, and found no significant changes to D1-MSN dendritic complexity compared to the water mice (FigS1D; water vs fentanyl-no-abstinence, p's>0.05 at all Sholl radiuses, branch points, total dendritic length). D2-MSN dendritic complexity remained unchanged by fentanyl exposure (FigS1E, p's>0.05).

Homecage fentanyl abstinence increases D1-MSN excitability and sEPSC amplitude

Reduced dendritic complexity is associated with altered excitability of D1-MSNs(57,58). Thus, we next assessed how fentanyl abstinence altered MSN physiology. We used AAV-DO-tdTomato-DIO-eGFP(62) in D1-Cre mice to label Cre-positive D1-MSNs in green, and Cre-negative D2-MSNs in red (Fig2A, representative site in Fig2B, drinking in FigS5H). Since opioid-induced electrophysiologic adaptations are NAc subregion-specific(23), we

restricted our analysis to cells in the NAc core, and at the core/shell boundary. Fentanyl abstinence did not alter the frequency of spontaneous excitatory post-synaptic currents (sEPSCs) onto D1-MSNs (Fig2C, p=0.187,nested t-test). Instead, we found abstinence increased median sEPSC amplitudes relative to D1-MSNs from water mice (Fig2D p=0.011, nested t-test), and caused a rightward shift in the cumulative probability plot(Fig2D Kolmogorov-Smirnov D=0.14,p=0.01). Fentanyl abstinence did not alter median sEPSC inter-event-interval (Fig2E, p=0.642,nested t-test), nor shift cumulative probability (D=0.01,p>0.99). Along with increased sEPSC amplitude, fentanyl abstinence caused a hyper-excitable phenotype in D1-MSNs marked by a more hyperpolarized action potential threshold(Fig2F,p=0.006, nested t-test) and a trend towards an increased number of current-evoked spikes(Fig2G Left:drug p=0.09, mixed-effects analysis; Right:p=0.07 nested t-test). Fentanyl abstinence did not alter sEPSC frequency onto D2-MSNs (Fig2H, p=0.467, nested t-test), nor significantly increase median sEPSC amplitudes or cumulative probability (Fig2I p=0.252, nested t-test; D=0.02, p>0.99). We found no differences in median sEPSC inter-event-interval, nor shifts in cumulative probability for D2-MSNs from fentanyl-abstinent mice (Fig2J p=0.624,nested t-test; D=0.098, p>0.99). D2-MSN excitability was unchanged by fentanyl abstinence as there were no differences in threshold potential (Fig2K,p=0.14, nested t-test) or current-evoked spikes (Fig2L Left: drug p=0.299, RMANOVA; Right: p=0.494,nested t-test). In both MSN-subtypes, fentanyl abstinence did not significantly change resting membrane properties(FigS2).

Fentanyl abstinence causes distinct changes to D1- and D2-MSN translatomes

To determine potential molecular mechanisms underlying D1-MSN specific atrophy and physiology changes, we extracted RNA from immunoprecipitated polyribosomes in D1-and D2-MSNs as in our previous work(56,63). We sequenced D1-and D2-MSN translatomes (Fig3A–B, drinking in FigS3A), and found little overlap in the differentially expressed genes between MSN-subtypes after fentanyl abstinence (Fig 3C). We used Nanostring to measure mRNA levels in D1-and D2-MSN translatomes and confirmed MSN subtype-specificity of our samples(FigS3B). Next, we performed Weighted Gene Co-Expression Network Analysis(WGCNA) in each MSN subtype. We identified 19 modules of co-expressed genes in D1-MSNs and 16 in D2-MSNs (Fig3D). From 35 total modules, we chose 11 for further exploration based on p<0.05 for effect of fentanyl (Fig3E;Table S1). The effects of fentanyl abstinence on module eigengene expression was primarily MSN-subtype-specific, except for Black and Red which contained upregulated or downregulated genes, respectively, in both subtypes. We next used Nanostring to assess differential expression of 3 randomly selected hub genes from each fentanyl module, and analyzed with sexes combined, and in each sex independently (Fig3G). Despite reduced sensitivity for detecting small expression changes, Nanostring analysis showed 16/33 selected hub genes were significantly differentially expressed in one or both sexes, and all tested hub genes were concordant with RNAseq data (i.e. up-or down-regulated by abstinence). To further refine the fentanyl modules, we performed Gene Ontology (GO) Analysis on the genes from each module using BiNGO(63,64)(Supplemental File 2). Given the changes to dendritic complexity and excitability, we looked for overrepresentation of synaptic and dendritic complexity GO terms(Fig4A), and found enrichment in Green and Magenta modules. We selected the Green module for further investigation since dendritic complexity loss was specific to D1-MSNs,

and the Green module contained genes downregulated in D1-MSNs (module structure in Fig3F). We measured expression of additional Green module genes with Nanostring(Fig4B), comparing across and between sexes. Several tested genes were significantly downregulated after fentanyl abstinence and were primarily restricted to D1-MSNs. Two Green module genes (*Cdk5r1* and *Nat8l*) were significantly changed in D2-MSNs from female mice. With sexes combined, we found significant downregulation of *Gramd1b*, *Nat8l*, and *Prkce*; with sexes separated, downregulated *Gramd1b* and *Prkce* reached statistical significance in males, and *Nat8l* in females(Fig4B). Many tested Green-Module genes were downregulated in D1-MSNs, but failed to reach statistical significance with sexes combined (*Kcnj11* p=0.071; *Syt7* p=0.085) and when comparing within sex (males: *Syt7* p=0.069; *Camk2n1* p=0.083; *Ddn* p=0.075; *Flna* p=0.064; females: *Pum2* p=0.078).

D1-MSN synaptic and dendritic complexity molecules share common transcriptional regulators

Given the variation in Green-Module gene downregulation between the sexes, we next looked for potential upstream transcriptional regulators. We used iRegulon(65) to look for transcription factor binding motifs enriched in the promoters of Hub genes in the Green-Module. This analysis identified 13 enriched sequence motifs (Supplemental File3). Of the transcription factors that recognize these motifs, E2F1 stood out because the *E2f1* gene was itself a member of the Green-Module, down-regulated following abstinence from fentanyl. Ten genes in the Green-Module were predicted as E2F1 targets based on the evolutionarily-conserved enrichment of E2F1 sequence motifs +/− 20 kb from their transcription start sites(Fig4C;Supplemental File3). From this gene list, we selected three predicted E2f1 targets for chromatin binding analysis with Cut & Run qPCR in mice that underwent fentanyl abstinence. Since this method used bulk NAc tissue, we did not detect statistically significant changes, however there was a trend for increased E2f1 binding upstream of *Nlgn2* in the fentanyl-abstinent condition (FigS3E,p=0.084, unpaired t-test).

Next, we sought to confirm our RNAseq results showing decreased E2f1 in D1-MSNs after abstinence. Nanostring revealed decreased E2f1 counts in fentanyl-abstinent D1-translatomes(Fig4D,p=0.05), but not D2-MSN translatomes (p=0.49). We replicated this with single molecule fluorescence *in situ* hybridization (RNAscope) in a separate cohort of D1-and A2A-Cre mice (Drinking in FigS3C). We used probes against E2f1 and Cre to identify *E2f1* mRNA in NAc core D1-or D2-MSNs. Although fentanyl abstinence did not alter the number of E2f1 expressing Cre positive nuclei in either MSN subtype, (Fig4F,p's>0.14) fentanyl abstinence was associated with a significant decrease in *E2f1* puncta per Cre-positive D1-MSN nucleus(Fig4G,p=0.028). By contrast, there were no significant differences in D2-MSNs, and a trend towards increased *E2f1* puncta in D2-MSNs from fentanyl-abstinent A2A-Cre mice(p=0.068).

Increased E2f1 in D1-MSNs protects against fentanyl abstinence-induced atrophy, plasticity, and behaviors

Since *E2f1* was decreased in D1-MSNs from fentanyl-abstinent mice, we made a Cre-inducible AAV to overexpress *E2f1* in D1-MSNs during fentanyl exposure(FigS4A–C). In Cre-transfected Neuro2A cells, we found AAV-DIO-E2f1 decreased levels of *E2f1*

target genes (Fig5A mRNA:Nlgn2, p=0.047, Gramd1b,p=0.0001; FigS4B protein:Nlgn2, p=0.038, Gramd1b, p=0.044). In D1-Cre mice expressing AAV-DIO-E2f1 (representative expression in Fig5B), there were trends towards decreased expression of target genes *Nlgn2* and *Gramd1b* in total NAc, likely due to *E2f1* manipulation in only a subset of neurons (FigS4D,p=0.085, p=0.09).

We next asked if E2f1 overexpression during abstinence could protect against D1-MSN dendritic atrophy and altered physiology. We co-infused AAV-DIO-E2f1 and DIO-eYFP in D1-Cre mice 3-weeks before fentanyl exposure (Fig5C, drinking in FigS4E). We found no differences in dendritic morphology between D1-MSNs in water or fentanyl abstinent mice expressing DIO-E2f1+eYFP (Representative D1-MSNs in Fig5D) as measured by Sholl intersections, number of branch points, and total dendritic length (Fig5E–G, p's>0.05). To ensure E2f1 did not affect baseline dendritic morphology, we compared E2f1+eYFP D1-MSNs to eYFP-only D1-MSNs(FigS4H–J). Sholl intersections from water/eYFP mice were indistinguishable from *both* water/E2f1+eYFP and fentanyl abstinent/E2f1+eYFP D1-MSNs (FigS4H). This was also true for branch points (FigS4I) and total dendritic length (FigS4J), indicating E2f1 protected D1-MSNs from abstinence-induced atrophy without impacting baseline morphology. Importantly, E2f1 did not protect against atrophy by significantly altering fentanyl consumption (FigS4E,p>0.05).

Next, we performed patch-clamp electrophysiology in D1-cre mice co-expressing AAV-DO-tdTomato-DIO-GFP and AAV-DIO-E2f1 (Fig5H, drinking in FigS5H). In mice expressing E2f1+eGFP, fentanyl abstinence did not increase median sEPSC amplitude (Fig5J, nested t-test p=0.49; D=0.038, p=0.99), threshold potential (Fig5K,p=0.233), nor number of AP's (Fig5L,p=0.75) relative to water/E2f1+eGFP mice, suggesting a protective effect of E2f1. To asses E2f1 effects on baseline physiology, we also compared E2f1+eGFP D1-MSNs to eGFP only D1-MSNs (FigS5). Neither water/E2f1+eGFP nor fentanyl/E2f1+eGFP had statistically different sEPSC amplitude compared with water/eGFP alone (FigS5C). E2f1 did not alter excitability as measured by threshold potential (FigS5E), however, we observed increased evoked APs per current injection (FigS5F, StepXVirus, p=0.05), and increased number of APs at 120 pA relative to water/eGFP D1-MSNs, (FigS5G, Virus p=0.037). Together, these data indicate E2f1 overexpression protects against abstinence-increased sEPSC amplitudes, but the effects on abstinence-induced hyperexcitability are unclear due to general E2f1 effects. Importantly, the physiological changes are not due to differences in consumption between eGFP and E2f1+eGFP groups (FigS5H,p>0.05).

Given that increased E2f1 expression protected against D1-MSN atrophy and changes to sEPSC amplitude, we next asked if it would protect against abstinence-induced negative affective behaviors. D1-Cre mice received intra-NAc AAV-DIO-E2f1 or AAV-DIO-eYFP 3-weeks before fentanyl drinking and abstinence (Fig5M). A subset of male mice underwent 1-day social defeat stress, while other males and females underwent EPM and 3-chamber social interaction tests, each separated by 24 hr. Only fentanyl-eYFP mice showed increased anxiety-like behavior (Fig5N, eYFP: water vs fentanyl-abstinence, p=0.002; E2f1: water vs fentanyl-abstinence, p=0.88) and reduced social interaction (Fig5O, eYFP:water vs fentanyl-abstinence, p=0.008; E2f1:water vs fentanyl-abstinence, p=0.98). We found E2f1 expression in D1-MSNs prevented stress-susceptibility in fentanyl abstinent male mice

subject to social stress (Fig5P, eYFP:water vs fentanyl-abstinence, p=0.003; E2f1:water vs fentanyl-abstinence, p=0.493). Importantly, E2f1 did not block behavioral effects by significantly altering fentanyl consumption(FigS4E–G).

Discussion

Here we show fentanyl abstinence induces neuron subtype-specific structural, functional, and molecular changes in the NAc. First, we found fentanyl abstinence increases anxiety-like behavior, social avoidance, and stress-susceptibility that is associated with a loss of D1-MSN dendritic complexity. Second, fentanyl abstinence increased D1-, but not D2-MSN excitability, and increased excitatory input onto D1-MSNs. These structural and functional changes were associated with altered expression of unique gene networks in each MSN subtype, including downregulation of transcriptionally co-regulated dendritic complexity and synaptic genes in D1-MSNs. Finally, increasing expression of transcriptional regulator E2f1 in D1-MSNs attenuated structural, functional, and behavioral changes caused by fentanyl abstinence.

The main goal of this study was to determine how fentanyl abstinence impacts NAc medium spiny neurons. Since NAc MSN morphology and physiology are stress-sensitive(56,66), we sought to minimize injection and handling stress by providing fentanyl in drinking water. Mice will reliably consume fentanyl-water in amounts similar to plain tap water(60). Because mice consume throughout the day, this method has the added benefit of mimicking intermittent drug use (vs continuous) and minimizing repeated bouts of withdrawal. We found fentanyl-exposed mice exhibited increased naloxone-precipitated withdrawal signs, suggesting our method produces a degree of opioid dependence. Similar to other protracted opioid abstinence studies(67–69), we found decreased social behavior and increased anxiety-like behavior in both sexes of abstinent mice. Since opioid-dependent individuals can exhibit increased HPA axis activation in response to stress(61), we also assessed stress-susceptibility in male mice using a subthreshold social stressor. This procedure measures stress-susceptibility in a short, open-field based test, and without additional manipulation, mice do not show social avoidance. If mice receive a “pro-stress” manipulation prior to subthreshold stress, they show increased social-avoidance of a novel CD-1. Using this procedure, we found fentanyl abstinence with subthreshold stress increased social-avoidance and stress-susceptibility. The unstressed fentanyl abstinent male mice did not show a significant decrease in interaction time in the open-field based test. This is likely due to the shorter testing duration, a different social target, and smaller arena vs the 3-chamber social interaction test. The decreased social-interaction we see in the longer 3-chamber test(Fig 1B) is concordant with our previous work showing reduced interaction in this test after 56 hr fentanyl abstinence(60).

Drugs with abuse potential alter NAc MSN morphology. Canonically, psychostimulants increase dendritic spine density, while opioids instead decrease spine density (28). Further, dopamine depletion has long been associated with a loss of MSN dendritic complexity and spine density(70,71), and opioid abstinence or withdrawal reduces NAc dopamine release(8–11). Opioid-induced spine loss and dendritic atrophy have been replicated across a number of morphine studies(21,26–28,31,72) (but see (32); however comparatively fewer

studies examine dendritic morphology changes in specific MSN subtypes (17). Here we found fentanyl abstinence reduced dendritic complexity in D1-MSNs, but not D2-MSNs. Further, preventing abstinence-induced D1-MSN dendritic atrophy was protective against increased negative affective behaviors. These findings resemble those of our chronic stress work where only D1-MSNs show reduced dendritic arborization, and preventing or reversing D1-MSN dendritic atrophy decreases negative affective behaviors in the context of chronic stress(56,58). Together our findings add to growing evidence for NAc D1-MSN's importance in the expression of affective behavior. Surprisingly, we found spine density was relatively unchanged after fentanyl abstinence. This is contrary to most classic opioid literature, as well as our chronic stress work showing increased D2-MSN spine density(73). However, spine density changes may occur at a different timepoint than we assessed. Indeed, spine density is increased in NAc MSNs 1 day after morphine conditioned place preference(74); unchanged after 5 days of non-contingent morphine, and decreased at 21 days withdrawal(21). D1-MSN dendritic spine density is also reduced shortly after drug-induced reinstatement to heroin seeking(17). Further work is needed to establish the precise timeline for any dendritic spine changes in MSN subtypes during fentanyl exposure and abstinence.

Opioid abstinence is also associated with physiological changes to NAc MSNs that depend on duration. Acute (3–4 days) morphine abstinence is associated with decreased intrinsic excitability(29). After protracted (10–14 days) morphine abstinence, excitatory drive is instead potentiated(22,24), consistent with our protracted fentanyl abstinence data in D1-MSNs. Recent studies have begun to assess how opioid abstinence alters excitatory transmission in specific NAc MSN subtypes. In D1-MSNs, 1-day morphine abstinence has little impact on excitatory input(20), while 10–14 days increases GluA2 lacking AMPA receptors and excitatory drive on D1-MSNs specifically in the shell(23,25). Here, we found 10-day fentanyl abstinence increases sEPSC amplitudes, hyperpolarizes the threshold potential, and produces a trend towards more spikes per current injection in NAc core D1-MSNs. While we found no significant changes to D2-MSN excitability or excitatory drive in fentanyl abstinence, these changes may be more robust at a different withdrawal timepoint as in ref(75), or occur predominately in NAc shell D2-MSNs(20,21,23,25). Our significant differences in NAc core D1-MSNs differ from the work of Hearing and colleagues, who identified changes specifically in the shell(23,25). It is likely that methodologic differences drive this discrepancy, including administration route and opioid type.

It is also worth mentioning that increased excitability in abstinence-atrophied D1-MSNs resembles increased excitability in stress-atrophied D1-MSNs(58,66), and downregulated D1-MSN *Nlgn2* is a shared feature of abstinence and chronic stress(76). But while abstinence and stress share D1-MSN atrophy and hyperexcitability, they diverge regarding altered excitatory input. Stress *decreases* excitatory input onto D1-MSNs(77), whereas fentanyl abstinence *increases* sEPSC amplitudes. Our fentanyl abstinence findings suggest plasticity that either increases D1-MSN excitability to compensate for a loss of excitatory inputs or decreases dendritic complexity to compensate for overexcitation. Identifying which specific glutamatergic inputs are strengthened or weakened onto D1-MSNs(78) in both conditions may aid in identifying mechanistic similarities and differences between chronic stress-and abstinence-induced plasticity.

Altered MSN morphology and physiology arise as a consequence of altered gene expression. Here, we found fentanyl abstinence altered both D1-and D2-MSN translatomes, but to a greater extent in D1-MSNs. Numerous studies have identified molecular changes in the NAc arising during opioid abstinence, or as a consequence of opioid use(12–18,79), including recent work in postmortem human brain(80). Some notable similarities arise between our findings, and those of recent publications: neuronal morphology related genes are downregulated across species and paradigm(14,18,79). Like our work in abstinent mice, Mayberry et al found downregulated Green module genes in the NAc of male morphine self-administering rats (e.g. *Neurl4*, *Grik5*, *Shank3*);Townsend and colleagues found decreased Green-Module gene *Camk2n1* in the NAc of female fentanyl self-administering rats. There are numerous differentially expressed genes in D2-MSNs, including the D2-MSN specific Magenta Module. Since our dendritic atrophy phenotype was restricted to D1-MSNs, we chose to focus on gene expression changes in D1-MSNs, however the D2-MSN expression changes may reflect adaptations which protect against increased dendritic spine density on D2-MSNs(73), or other dendritic complexity changes. There are several promising targets for future investigation in the Magenta Module, including 2 hub genes that are transcription factors (*Arx*, *Dlx1*). Recapitulating changes to D2-MSN translatomes in D1-MSNs may also represent an additional opportunity to block dendritic atrophy.

To establish a role for the Green Module in mediating D1-MSN atrophy, we selected transcription factor E2f1 for further investigation. Our iRegulon analysis predicted E2f1 regulated many Green Module genes (including 5 hub genes) and E2f1 was also downregulated by fentanyl abstinence. Further, globally disrupting E2f1-DNA binding increases anxiety-like behavior(81), consistent with our behavioral findings. The E2f family is known to regulate gene expression following cocaine(82–84), and their transcriptional activity can be influenced by opioid receptor activation(85). Outside of the brain, E2f1 is primarily nuclear where it serves to regulate the cell cycle; however in post-mitotic neurons, E2f1 is found in the cytoplasm—especially in neuronal processes(81,86). Despite its odd localization, E2f1 binds to several gene promoters in cortical neurons, most notably DNA repair related genes following DNA damage(87). Here, we find increasing E2f1 expression in N2a cells results in decreased expression of two target genes *Nlgn2* and *Gramd1b*. At first, this seems at odds with our finding that increased E2f1 in D1-MSNs protects against abstinence-induced dendritic atrophy, since it should theoretically work by *preventing* downregulation of those same genes. However, E2f1 function has been poorly characterized in the intact brain, and its function in neuronal cytoplasm is undetermined. In our iRegulon analysis, we also found E2f1 contains at least one E2f1 motif, and our viral expression may have induced self-regulation. Thus, E2f1 overexpression may protect against dendritic atrophy but potentially engages mechanisms of self-regulation to maintain homeostasis in D1-MSNs by dampening select E2f1 targets. Coincidentally, abstinence from morphine self-administration was recently shown to downregulate genes with E2f1 binding motifs(14), and may thus be a way to manipulate maladaptive gene expression for both natural and synthetic opioids.

Lastly, aside from the Green Module genes associated with dendritic complexity, there are other candidate genes in the module that may drive altered D1-MSN physiology. For hyperexcitability, this list includes downregulated expression of K_v subunit genes

Kcna2, *Kcnb1*, and *Kcnq4*. We also found decreased expression of E2f1 target *Kcnj11*, an ATP-sensitive K+channel subunit, although this did not reach statistical significance with Nanostring (p=0.07). While promising, the effect of Kcnj11 on hyperexcitability will need to be tested directly since increased E2f1 may have shifted D1-MSN excitability by altering other molecular targets. Additional downregulated voltage gated channel activity genes are found in the Red Module (e.g. *Kcnb2*, *Hcn4*; see Supplemental File 2). For increased sEPSC amplitudes, the potential direct molecular mediators are less clear as the list of differentially expressed kinases, phosphatases, and their regulators is long. Further, enzymes important for receptor trafficking and post-translational modification are Ca2+ sensitive and often interdependent. For example, Green Module gene and E2f1-target *Camk2n1* may have diverse effects depending on where in the cell it inhibits CaMKII or alters Ca2+ homeostasis. In the future, subtype-specific chromatin profiling will enable us to more precisely identify E2f1 target genes in the intact brain, helping to narrow the list of candidates responsible for each morphologic and physiologic effect.

Together, our findings illustrate that a single bout of protracted fentanyl abstinence can produce structural, functional, and molecular changes in the brain, and these changes contribute to an increase in negative affective symptoms. Individuals with opioid use disorder oscillate between periods of drug use and abstinence, likely magnifying these neural adaptations. Targeting the molecular mechanisms during the transition from opioid use to abstinence may provide an important new therapeutic avenue. Intervention during this period may prevent some of the neurobiological changes, along with reducing negative-affective symptoms driving relapse and overdose.

Supplementary Material

Refer to Web version on PubMed Central for supplementary material.

Funding and acknowledgements

This study was funded by NIH K99/R00 DA050575 to MEF; R01MH106500, R01DA047943, R21DA052101, R21DA048554 and R01DA38613 to MKL; R01 MH086828 to SMT. A previous version of this manuscript was deposited to bioRxiv at https://doi.org/10.1101/2022.05.15.491856

References

1. Drug Enforcement Administration (2016): Counterfeit prescription pills containing fentanyls: A global threat. DEA Intelligence Brief. Retrieved April 13, 2022, from https://www.safemedicines.org/2018/06/fentanyl-has-created-a-new-kind-of-21st-century-drug-kingpin.html
2. Ahmad F, Rossen L, Sutton P (2021): Provisional drug overdose death counts. National Center for Health Statistics. Des by LM Rossen, A Lipphardt, FB Ahmad, JM Keralis, Y Chong Natl Cent Heal Stat. Retrieved from https://www.cdc.gov/nchs/nvss/vsrr/drug-overdose-data.htm
3. Volkow ND, Koob GF, McLellan AT (2016): Neurobiologic Advances from the Brain Disease Model of Addiction. N Engl J Med 374: 363–371. [PubMed: 26816013]
4. Koob GF (2020): Neurobiology of Opioid Addiction: Opponent Process, Hyperkatifeia, and Negative Reinforcement. Biol Psychiatry 87: 44–53. [PubMed: 31400808]
5. Jordan CJ, Xi ZX (2022): Identification of the Risk Genes Associated With Vulnerability to Addiction: Major Findings From Transgenic Animals. Front Neurosci 15. 10.3389/FNINS.2021.811192

6. Reiner DJ, Fredriksson I, Lofaro OM, Bossert JM, Shaham Y (2019, February 6): Relapse to opioid seeking in rat models: behavior, pharmacology and circuits. Neuropsychopharmacology, vol. 44. Nature Publishing Group, pp 465–477. [PubMed: 30293087]
7. Browne CJ, Godino A, Salery M, Nestler EJ (2020, January 1): Epigenetic Mechanisms of Opioid Addiction. Biological Psychiatry, vol. 87. Elsevier USA, pp 22–33. [PubMed: 31477236]
8. Rossetti ZL, Hmaidan Y, Gessa GL (1992): Marked inhibition of mesolimbic dopamine release: a common feature of ethanol, morphine, cocaine and amphetamine abstinence in rats. Eur J Pharmacol 221: 227–234. [PubMed: 1426002]
9. Acquas E, Carboni E, Di Chiara G (1991): Profound depression of mesolimbic dopamine release after morphine withdrawal in dependent rats. Eur J Pharmacol 193: 133–134. [PubMed: 1646728]
10. Pothos E, Rada P, Mark GP, Hoebel BG (1991): Dopamine microdialysis in the nucleus accumbens during acute and chronic morphine, naloxone-precipitated withdrawal and clonidine treatment. Brain Res 566: 348–350. [PubMed: 1814554]
11. Fox ME, Nathan Rodeberg T, Mark Wightman R, Rodeberg NT, Wightman RM (2017): Reciprocal Catecholamine Changes during Opiate Exposure and Withdrawal. Neuropsychopharmacology 42: 671–681. [PubMed: 27461081]
12. Cahill ME, Browne CJ, Wang J, Hamilton PJ, Dong Y, Nestler EJ (2018): Withdrawal from repeated morphine administration augments expression of the RhoA network in the nucleus accumbens to control synaptic structure. J Neurochem 147: 84–98. [PubMed: 30071134]
13. Sun HS, Martin JA, Werner CT, Wang ZJ, Damez-Werno DM, Scobie KN, et al. (2016): BAZ1B in nucleus accumbens regulates reward-related behaviors in response to distinct emotional stimuli. J Neurosci 36: 3954–3961. [PubMed: 27053203]
14. Mayberry HL, Bavley CC, Karbalaei R, Peterson DR, Bongiovanni AR, Ellis AS, et al. (2022): Transcriptomics in the nucleus accumbens shell reveal sex- and reinforcer-specific signatures associated with morphine and sucrose craving. Neuropsychopharmacology. 10.1038/S41386-022-01289-2
15. Ferguson D, Koo JW, Feng J, Heller E, Rabkin J, Heshmati M, et al. (2013): Essential role of SIRT1 signaling in the nucleus accumbens in cocaine and morphine action. J Neurosci 33: 16088–16098. [PubMed: 24107942]
16. Spijker S, Houtzager SWJ, De Gunst MCM, De Boer WPH, Schoffelmeer ANM, Smit AB (2004): Morphine exposure and abstinence define specific stages of gene expression in the rat nucleus accumbens. FASEB J 18: 848–850. [PubMed: 15033927]
17. Martin JA, Werner CT, Mitra S, Zhong P, Wang ZJ, Gobira PH, et al. (2019): A novel role for the actin-binding protein drebrin in regulating opiate addiction. Nat Commun 10: 4140. [PubMed: 31515501]
18. Townsend EA, Kim RK, Robinson HL, Marsh SA, Banks ML, Hamilton PJ (2021): Opioid withdrawal produces sex-specific effects on fentanyl-vs.-food choice and mesolimbic transcription. Biol psychiatry Glob open Sci 1: 112. [PubMed: 34458885]
19. Hofford RS, Mervosh NL, Euston TJ, Meckel KR, Orr AT, Kiraly DD (2021): Alterations in microbiome composition and metabolic byproducts drive behavioral and transcriptional responses to morphine. Neuropsychopharmacology 46: 2062–2072. [PubMed: 34127799]
20. McDevitt DS, Jonik B, Graziane NM (2019): Morphine Differentially Alters the Synaptic and Intrinsic Properties of D1R- and D2R-Expressing Medium Spiny Neurons in the Nucleus Accumbens. Front Synaptic Neurosci 11. 10.3389/fnsyn.2019.00035
21. Graziane NM, Sun S, Wright WJ, Jang D, Liu Z, Huang YH, et al. (2016): Opposing mechanisms mediate morphine- and cocaine-induced generation of silent synapses. Nat Neurosci 19: 915–925. [PubMed: 27239940]
22. Wu X, Shi M, Ling H, Wei C, Liu Y, Liu Z, Ren W (2013): Effects of morphine withdrawal on the membrane properties of medium spiny neurons in the nucleus accumbens shell. Brain Res Bull 90: 92–99. [PubMed: 23069789]
23. Madayag AC, Gomez D, Anderson EM, Ingebretson AE, Thomas MJ, Hearing MC (2019): Cell-type and region-specific nucleus accumbens AMPAR plasticity associated with morphine reward, reinstatement, and spontaneous withdrawal. Brain Struct Funct 224: 2311–2324. [PubMed: 31201496]

24. Wu X, Shi M, Wei C, Yang M, Liu Y, Liu Z, et al. (2012): Potentiation of synaptic strength and intrinsic excitability in the nucleus accumbens after 10 days of morphine withdrawal. J Neurosci Res 90: 1270–1283. [PubMed: 22388870]
25. Hearing MC, Jedynak J, Ebner SR, Ingebretson A, Asp AJ, Fischer RA, et al. (2016): Reversal of morphine-induced cell-type-specific synaptic plasticity in the nucleus accumbens shell blocks reinstatement. Proc Natl Acad Sci U S A 113: 757–762. [PubMed: 26739562]
26. Spiga S, Puddu MC, Pisano M, Diana M (2005): Morphine withdrawal-induced morphological changes in the nucleus accumbens. Eur J Neurosci 22: 2332–2340. [PubMed: 16262671]
27. Diana M, Spiga S, Acquas E (2006): Persistent and reversible morphine withdrawal-induced morphological changes in the nucleus accumbens. Annals of the New York Academy of Sciences, vol. 1074 1074: 446–457. [PubMed: 17105943]
28. Robinson TE, Kolb B (2004): Structural plasticity associated with exposure to drugs of abuse. Neuropharmacology 47: 33–46. [PubMed: 15464124]
29. Heng L-J, Yang J, Liu Y-H, Wang W-T, Hu S-J, Gao G-D (2008): Repeated morphine exposure decreased the nucleus accumbens excitability during short-term withdrawal. Synapse 62: 775–782. [PubMed: 18655119]
30. Thompson BL, Oscar-Berman M, Kaplan GB (2021, January 1): Opioid-induced structural and functional plasticity of medium-spiny neurons in the nucleus accumbens. Neuroscience and Biobehavioral Reviews, vol. 120. Elsevier Ltd, pp 417–430. [PubMed: 33152423]
31. Matsubara T, Matsuo K, Nakashima M, Nakano M, Harada K, Watanuki T, et al. (1999): Morphine alters the structure of neurons in the nucleus accumbens and neocortex of rats. Synapse 85: 160–162.
32. Pal A, Das S (2013): Chronic morphine exposure and its abstinence alters dendritic spine morphology and upregulates Shank1. Neurochem Int 62: 956–964. [PubMed: 23538264]
33. Gerfen CR, Surmeier DJ (2011): Modulation of Striatal Projection Systems by Dopamine. Annu Rev Neurosci 34: 441–466. [PubMed: 21469956]
34. Kupchik YM, Brown RM, Heinsbroek JA, Lobo MK, Schwartz DJ, Kalivas PW (2015): Coding the direct/indirect pathways by D1 and D2 receptors is not valid for accumbens projections. Nat Neurosci 18: 1230–1232. [PubMed: 26214370]
35. Smith RJ, Lobo MK, Spencer S, Kalivas PW (2013, August): Cocaine-induced adaptations in D1 and D2 accumbens projection neurons (a dichotomy not necessarily synonymous with direct and indirect pathways). Current Opinion in Neurobiology, vol. 23. pp 546–552. [PubMed: 23428656]
36. Calipari ES, Bagot RC, Purushothaman I, Davidson TJ, Yorgason JT, Peña CJ, et al. (2016): In vivo imaging identifies temporal signature of D1 and D2 medium spiny neurons in cocaine reward. Proc Natl Acad Sci 113: 2726–2731. [PubMed: 26831103]
37. Lobo MK, Covington HE, Chaudhury D, Friedman AK, Sun HS, Damez-Werno D, et al. (2010): Cell type - Specific loss of BDNF signaling mimics optogenetic control of cocaine reward. Science (80-) 330: 385–390.
38. Hauser SR, Deehan GA, Dhaher R, Knight CP, Wilden JA, McBride WJ, Rodd ZA (2015): D1 receptors in the nucleus accumbens-shell, but not the core, are involved in mediating ethanol-seeking behavior of alcohol-preferring (P) rats. Neuroscience 295: 243–251. [PubMed: 25813708]
39. Koo JW, Lobo MK, Chaudhury D, Labonté B, Friedman A, Heller E, et al. (2014): Loss of BDNF signaling in D1R-expressing NAc neurons enhances morphine reward by reducing GABA inhibition. Neuropsychopharmacology 39: 2646–2653. [PubMed: 24853771]
40. Kravitz AV, Tye LD, Kreitzer AC (2012): Distinct roles for direct and indirect pathway striatal neurons in reinforcement. Nat Neurosci 15: 816–818. [PubMed: 22544310]
41. James AS, Chen JY, Cepeda C, Mittal N, Jentsch JD, Levine MS, et al. (2013): Opioid self-administration results in cell-type specific adaptations of striatal medium spiny neurons. Behav Brain Res 256: 279–283. [PubMed: 23968589]
42. Hikida T, Kimura K, Wada N, Funabiki K, Nakanishi S (2010): Distinct roles of synaptic transmission in direct and indirect striatal pathways to reward and aversive behavior. Neuron 66: 896–907. [PubMed: 20620875]

43. Tai LH, Lee AM, Benavidez N, Bonci A, Wilbrecht L (2012): Transient stimulation of distinct subpopulations of striatal neurons mimics changes in action value. Nat Neurosci 15: 1281–1289. [PubMed: 22902719]
44. Gallo EF, Meszaros J, Sherman JD, Chohan MO, Teboul E, Choi CS, et al. (2018): Accumbens dopamine D2 receptors increase motivation by decreasing inhibitory transmission to the ventral pallidum. Nat Commun 9. 10.1038/s41467-018-03272-2
45. Soares-Cunha C, Coimbra B, David-Pereira A, Borges S, Pinto L, Costa P, et al. (2016): Activation of D2 dopamine receptor-expressing neurons in the nucleus accumbens increases motivation. Nat Commun 7: 11829. [PubMed: 27337658]
46. Soares-Cunha C, de Vasconcelos NAP, Coimbra B, Domingues AV, Silva JM, Loureiro-Campos E, et al. (2019): Nucleus accumbens medium spiny neurons subtypes signal both reward and aversion. Mol Psychiatry 1–15.
47. Gibson GD, Prasad AA, Jean-Richard-dit-Bressel P, Yau JOY, Millan EZ, Liu Y, et al. (2018): Distinct Accumbens Shell Output Pathways Promote versus Prevent Relapse to Alcohol Seeking. Neuron 98: 512–520.e6. [PubMed: 29656870]
48. Natsubori A, Tsutsui-Kimura I, Nishida H, Bouchekioua Y, Sekiya H, Uchigashima M, et al. (2017): Ventrolateral striatal medium spiny neurons positively regulate food-incentive, goal-directed behavior independently of D1 and D2 selectivity. J Neurosci 37: 2723–2733. [PubMed: 28167674]
49. Cui G, Jun SB, Jin X, Pham MD, Vogel SS, Lovinger DM, Costa RM (2013): Concurrent Activation of Striatal Direct and Indirect Pathways During Action Initiation. Nature 494: 238. [PubMed: 23354054]
50. Soares-Cunha C, Coimbra B, Domingues AV, Vasconcelos N, Sousa N, Rodrigues AJ (2018): Nucleus Accumbens Microcircuit Underlying D2-MSN-Driven Increase in Motivation. eNeuro 5. 10.1523/ENEURO.0386-18.2018
51. Vicente AM, Galvão-Ferreira P, Tecuapetla F, Costa RM (2016): Direct and indirect dorsolateral striatum pathways reinforce different action strategies. Curr Biol 26: R267–R269. [PubMed: 27046807]
52. Engeln M, Fox ME, Lobo MK (2021): Housing conditions during self-administration determine motivation for cocaine in mice following chronic social defeat stress. Psychopharmacology (Berl) 238: 41–54. [PubMed: 32914243]
53. Kennedy BC, Panksepp JB, Runckel PA, Lahvis GP (2012): Social influences on morphine-conditioned place preference in adolescent BALB/cJ and C57BL/6J mice. Psychopharmacology (Berl) 219: 923–932. [PubMed: 21837434]
54. Bozarth MA, Murray A, Wise RA (1989): Influence of housing conditions on the acquisition of intravenous heroin and cocaine self-administration in rats. Pharmacol Biochem Behav 33: 903–907. [PubMed: 2616610]
55. Westenbroek C, Perry AN, Becker JB (2013): Pair housing differentially affects motivation to self-administer cocaine in male and female rats. Behav Brain Res 252: 68–71. [PubMed: 23727175]
56. Fox ME, Chandra R, Menken MS, Larkin EJ, Nam H, Engeln M, et al. (2020): Dendritic remodeling of D1 neurons by RhoA/Rho-kinase mediates depression-like behavior. Mol Psychiatry 25: 1022–1034. [PubMed: 30120419]
57. Francis TC, Gaynor A, Chandra R, Fox ME, Lobo MK (2019): The Selective RhoA Inhibitor Rhosin Promotes Stress Resiliency Through Enhancing D1-Medium Spiny Neuron Plasticity and Reducing Hyperexcitability. Biol Psychiatry 85: 1001–1010. [PubMed: 30955841]
58. Francis TC, Chandra R, Gaynor A, Konkalmatt P, Metzbower SR, Evans B, et al. (2017): Molecular basis of dendritic atrophy and activity in stress susceptibility. Mol Psychiatry 22: 1512–1519. [PubMed: 28894298]
59. Ueno H, Takahashi Y, Suemitsu S, Murakami S, Kitamura N, Wani K, et al. (2020): Effects of repetitive gentle handling of male C57BL/6NCrl mice on comparative behavioural test results. Sci Reports 2020 101 10: 1–13.
60. Franco D, Wulff AB, Lobo MK, Fox ME (2022): Chronic Physical and Vicarious Psychosocial Stress Alter Fentanyl Consumption and Nucleus Accumbens Rho GTPases in Male and Female C57BL/6 Mice. Front Behav Neurosci 16. 10.3389/fnbeh.2022.821080

61. Wemm SE, Sinha R (2019): Drug-induced stress responses and addiction risk and relapse. Neurobiol Stress 10: 100148. [PubMed: 30937354]

62. Saunders A, Johnson CA, Sabatini BL (2012): Novel recombinant adeno-associated viruses for Cre activated and inactivated transgene expression in neurons. Front Neural Circuits 6. 10.3389/FNCIR.2012.00047

63. Engeln M, Song Y, Chandra R, La A, Fox MEME, Evans B, et al. (2020): Individual differences in stereotypy and neuron subtype translatome with TrkB deletion. Mol Psychiatry 26: 1–14.

64. Maere S, Heymans K, Kuiper M (2005): BiNGO: A Cytoscape plugin to assess overrepresentation of Gene Ontology categories in Biological Networks. Bioinformatics 21: 3448–3449. [PubMed: 15972284]

65. Janky R, Verfaillie A, Imrichová H, Sande B Van de, Standaert L, Christiaens V (2014): PLoS Comput Biol. PLoS Computational Biology, vol. 10. Public Library of Science, p e1003731. [PubMed: 25058159]

66. Francis TC, Chandra R, Friend DM, Finkel E, Dayrit G, Miranda J, et al. (2015): Nucleus accumbens medium spiny neuron subtypes mediate depression-related outcomes to social defeat stress. Biol Psychiatry 77: 212–222. [PubMed: 25173629]

67. Bai Y, Li Y, Lv Y, Liu Z, Zheng X (2014): Complex motivated behaviors for natural rewards following a binge-like regimen of morphine administration: mixed phenotypes of anhedonia and craving after short-term withdrawal. Front Behav Neurosci 8: 23. [PubMed: 24550799]

68. Becker JAJ, Kieffer BL, Le Merrer J (2017): Differential behavioral and molecular alterations upon protracted abstinence from cocaine versus morphine, nicotine, THC and alcohol. Addict Biol 22: 1205–1217. [PubMed: 27126842]

69. Bravo IM, Luster BR, Flanigan ME, Perez PJ, Cogan ES, Schmidt KT, McElligott ZA (2020): Divergent behavioral responses in protracted opioid withdrawal in male and female C57BL/6J mice. Eur J Neurosci 51: 742–754. [PubMed: 31544297]

70. Ingham CA, Hood SH, Arbuthnott GW (1989): Spine density on neostriatal neurones changes with 6-hydroxydopamine lesions and with age. Brain Res 503: 334–338. [PubMed: 2514009]

71. Meredith GE, Ypma P, Zahm DS (1995): Effects of dopamine depletion on the morphology of medium spiny neurons in the shell and core of the rat nucleus accumbens. J Neurosci 15: 3808–3820. [PubMed: 7751948]

72. Leite-Morris KA, Kobrin KL, Guy MD, Young AJ, Heinrichs SC, Kaplan GB (2014): Extinction of opiate reward reduces dendritic arborization and c-Fos expression in the nucleus accumbens core. Behav Brain Res 263: 51–59. [PubMed: 24406724]

73. Fox ME, Figueiredo A, Menken MS, Lobo MK (2020): Dendritic spine density is increased on nucleus accumbens D2 neurons after chronic social defeat. Sci Rep 10: 12393. [PubMed: 32709968]

74. Kobrin KL, Moody O, Arena DT, Moore CF, Heinrichs SC, Kaplan GB (2016): Acquisition of morphine conditioned place preference increases the dendritic complexity of nucleus accumbens core neurons. Addict Biol 21: 1086–1096. [PubMed: 26096355]

75. Zhu Y, Wienecke CFR, Nachtrab G, Chen X (2016): A thalamic input to the nucleus accumbens mediates opiate dependence. Nature 530: 219–222. [PubMed: 26840481]

76. Heshmati M, Aleyasin H, Menard C, Christoffel DJ, Flanigan ME, Pfau ML, et al. (2018): Cell-type-specific role for nucleus accumbens neuroligin-2 in depression and stress susceptibility. Proc Natl Acad Sci U S A 115: 1111–1116. [PubMed: 29339486]

77. Francis TC, Lobo MK (2017): Emerging Role for Nucleus Accumbens Medium Spiny Neuron Subtypes in Depression. Biol Psychiatry 81: 645–653. [PubMed: 27871668]

78. LeGates TA, Kvarta MD, Tooley JR, Francis TC, Lobo MK, Creed MC, Thompson SM (2018): Reward behaviour is regulated by the strength of hippocampus–nucleus accumbens synapses. Nature 564: 258–262. [PubMed: 30478293]

79. Lefevre EM, Pisansky MT, Toddes C, Baruffaldi F, Pravetoni M, Tian L, et al. (2020): Interruption of continuous opioid exposure exacerbates drug-evoked adaptations in the mesolimbic dopamine system. Neuropsychopharmacology 45: 1–13.

80. Seney ML, Kim SM, Glausier JR, Hildebrand MA, Xue X, Zong W, et al. (2021): Transcriptional Alterations in Dorsolateral Prefrontal Cortex and Nucleus Accumbens Implicate

Neuroinflammation and Synaptic Remodeling in Opioid Use Disorder. Biol Psychiatry 90: 550–562. [PubMed: 34380600]

81. Ting JH, Marks DR, Schleidt SS, Wu JN, Zyskind JW, Lindl KA, et al. (2014): Targeted gene mutation of E2F1 evokes age-dependent synaptic disruption and behavioral deficits. J Neurochem 129: 850–863. [PubMed: 24460902]
82. Cates HM, Heller EA, Lardner CK, Purushothaman I, Peña CJ, Walker DM, et al. (2018): Transcription Factor E2F3a in Nucleus Accumbens Affects Cocaine Action via Transcription and Alternative Splicing. Biol Psychiatry 84: 167–179. [PubMed: 29397901]
83. Cates HM, Lardner CK, Bagot RC, Neve RL, Nestler EJ (2019): Fosb Induction in Nucleus Accumbens by Cocaine Is Regulated by E2F3a. eNeuro 6. 10.1523/ENEURO.0325-18.2019
84. Feng J, Wilkinson M, Liu X, Purushothaman I, Ferguson D, Vialou V, et al. (2014): Chronic cocaine-regulated epigenomic changes in mouse nucleus accumbens. Genome Biol 15. 10.1186/GB-2014-15-4-R65
85. Tencheva ZS, Praskova MD, Velichkova AA, Mitev VI (2005): δ-Opioid agonist induced regulation of E2F1 DNA binding activity in NG108–15 cells. Mol Brain Res 136: 271–274. [PubMed: 15893610]
86. Wang Y, Shyam N, Ting JH, Akay C, Lindl KA, Jordan-Sciutto KL (2010): E2F1 localizes predominantly to neuronal cytoplasm and fails to induce expression of its transcriptional targets in Human Immunodeficiency Virus-induced neuronal damage. Neurosci Lett 479: 97. [PubMed: 20580656]
87. Zhang Y, Song X, Herrup K (2020): Context-Dependent Functions of E2F1: Cell Cycle, Cell Death, and DNA Damage Repair in Cortical Neurons. Mol Neurobiol 57: 2377–2390. [PubMed: 32062842]

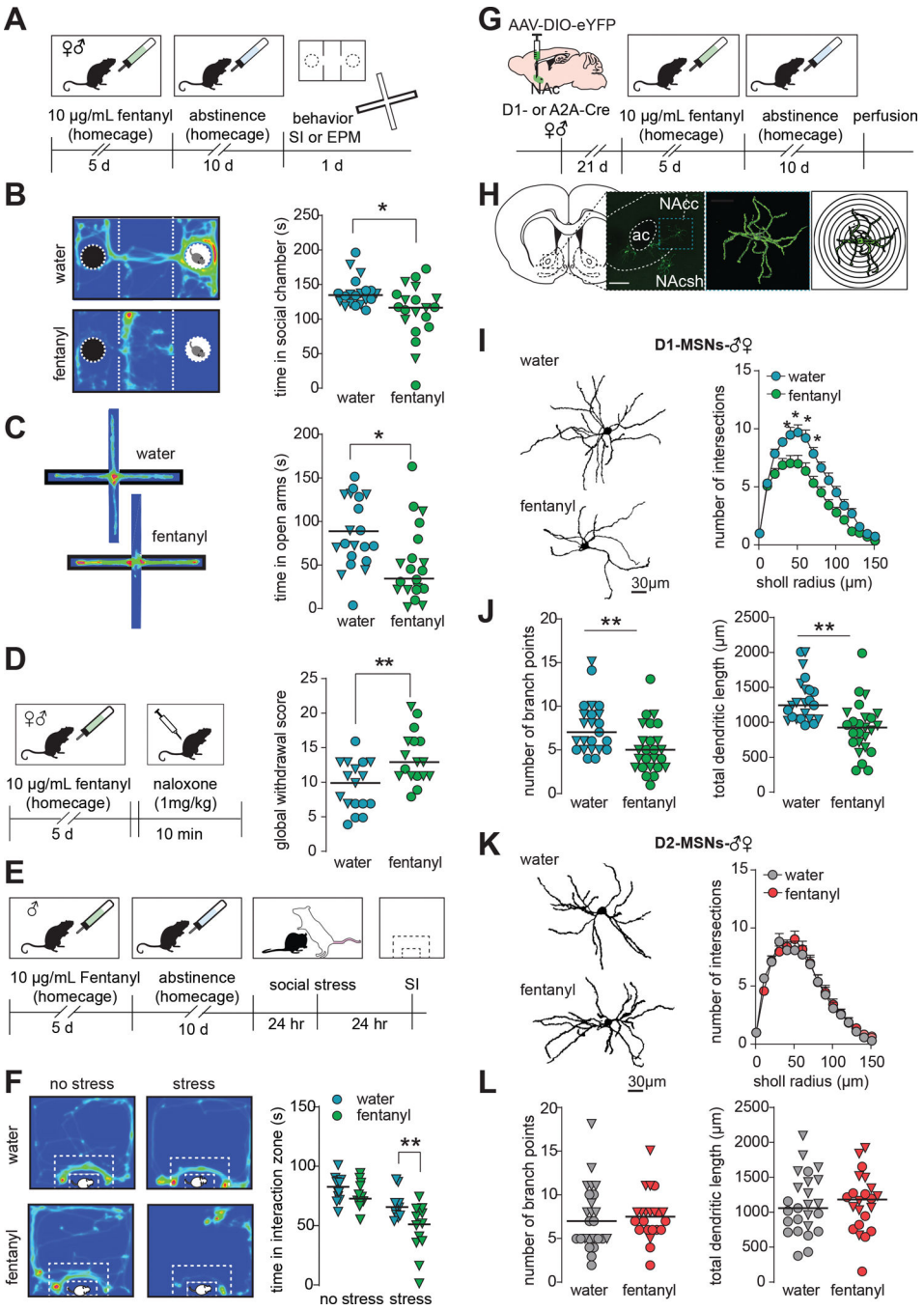

Figure 1. Fentanyl abstinence increases negative emotional behaviors and reduces dendritic complexity of D1-MSNs.

(**A**) Timeline for homecage fentanyl abstinence paradigm. Male and female mice received 10µg/mL fentanyl in drinking water for 5 days, then underwent 10 days of abstinence. Mice then underwent either social interaction (SI) or elevated plus maze (EPM) testing. (**B**) *Left*: example heat maps showing time a water or fentanyl abstinent mouse spent in the 3-chamber social interaction chamber when a novel mouse was present in the rightmost chamber. Warmer colors indicate increased duration. *Right*: Median and individual data

points showing time spent in the social chamber in water or fentanyl abstinent mice with a social target present (*, p=0.0165). Males are represented as triangles. (**C**) *Left*: example heat maps showing time a water or fentanyl abstinent mouse spent in the open and closed arms of an elevated plus maze. The closed arms are denoted by the thick black border. *Right*: Median and individual data points showing time spent in the open arms of the EPM (*, p=0.008). Males are represented as triangles. (**D**) *Left*: timeline for naloxone-precipitated withdrawal testing. Following 5 days of homecage fentanyl, mice received 1 mg/kg naloxone and were observed for withdrawal signs. *Right*: Median and individual data points showing global withdrawal scores in water or fentanyl mice given naloxone (**, p=0.0021). Males are represented as triangles. (**E**) Timeline for stress-susceptibility testing. After homecage fentanyl abstinence, male mice underwent a 1-day social stress paradigm in which they were subject to 3 brief agonistic encounters with 3 separate aggressive CD-1 residents separated by 10 min of sensory interaction. 24hr after stress, mice were assessed for social avoidance in an open field based social interaction (SI) test. (**F**) *Left*: example heat maps showing time unstressed and stressed water or fentanyl mice spent interacting with a novel CD-1. White dashed lines indicate interaction zone. *Right*: Median and individual data points showing time spent interacting with the social target (**, p=0.0017, Sidak's post-hoc after 2-way ANOVA). (**G**) Schematic of sparse-labeling approach of D1- and D2-MSNs. D1- or A2A-Cre mice underwent stereotaxic surgery for infusion of a Cre-dependent eYFP virus in the NAc to label D1- or D2 MSNs, respectively. Tissue slices containing the NAc were collected after homecage fentanyl abstinence. (**H**) Representative image of sparsely labeled MSNs in the NAc, a single MSN after 3D reconstruction, and concentric rings for Sholl analysis. (**I**) Representative D1-MSNs and Sholl analysis from water and fentanyl abstinent mice (mean ± sem;*,p<0.05 Sidak's post-hoc, n=48 cells from 18 mice). (**J**) Number of branch points and total dendritic length in D1-MSNs from water and fentanyl abstinent mice (**, p<0.005 nested t-test; n=48 cells from 18 mice; lines indicate median, males represented as triangles). (**K**) Representative D2-MSNs and Sholl analysis (mean ± sem), (**L**) number of branch points and total dendritic length in D2-MSNs from water and fentanyl abstinent mice. (p>0.05, n=47 cells from 17 mice; lines indicate median, males represented as triangles). See also Fig S1. Detailed statistics in Supplemental File 1.

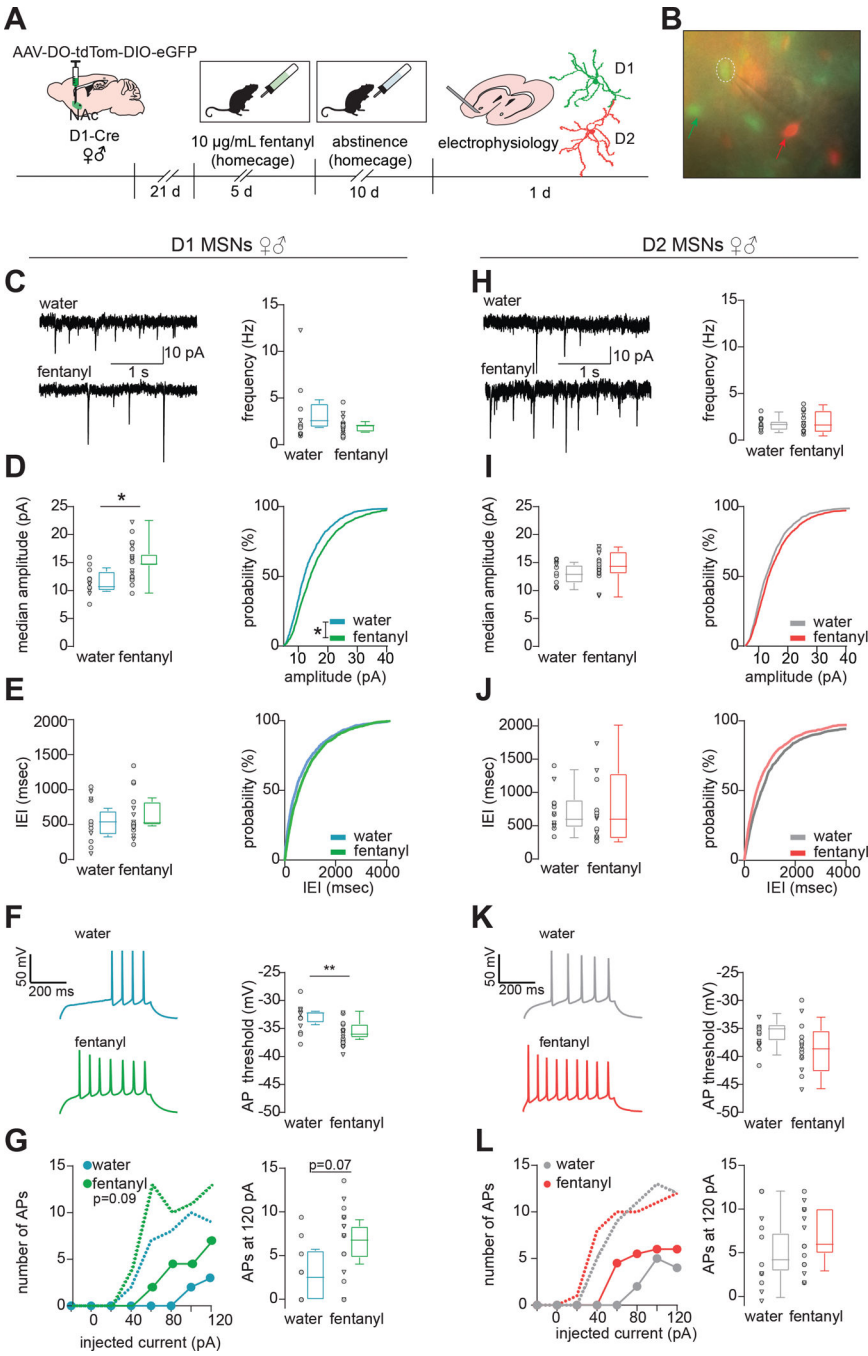

Figure 2. Fentanyl-abstinence increases D1-MSN excitatory input and excitability

(A) Schematic of MSN subtype labeling approach for electrophysiology experiments. Male and female D1-Cre mice received intra-NAc infusion of AAV-DO-TdTomato-DIO-eGFP virus so that Cre negative (i.e. D2-MSNs) express TdTomato, and Cre positive (D1-MSNs) express eGFP. Following homecage fentanyl abstinence, slices containing the NAc were collected for patch-clamp recording. (**B**) Representative image of MSN identification by red and green fluorescence prior to patching. Green and red arrows indicate D1- and D2-MSNs, respectively, patched D1-MSN denoted by hashed circle. (**C**) Spontaneous

excitatory postsynaptic currents (sEPSCs) were recorded while holding the membrane potential at −50 mV and analyzed by template-based event detection. Representative sEPSCs and median sEPSC frequency, (**D**) median sEPSC amplitude and cumulative probability (*, p=0.012 nested t-test; *, p=0.01, Kolmogrov-Smirnov D=0.14), (**E**) median sEPSC inter-event-interval (IEI) and cumulative probability in D1-MSNs from water and fentanyl abstinent mice. Individual data points represent individual neurons; triangles denote neurons from males. Box and whiskers plots show the median and range for data nested by mouse (n=28 cells from 12 mice). (**F**) Representative evoked action potentials (APs) and the potential required to elicit an AP, (**G**) number of APs elicited by injecting current in 20 pA intervals (median + range, circles and dashed lines, respectively), and number of APs at 120pA in D1-MSNs from water or fentanyl abstinent mice (n=23 cells from 10 mice, p=0.07, nested t-test). (**H**) Representative sEPSCs and median sEPSC frequency, (**I**) median sEPSC amplitude and cumulative probability, (**J**) median sEPSC inter-event-interval and cumulative probability in D2-MSNs from water and fentanyl abstinent mice (n=26 cells from 18 mice). (**K**) Representative evoked APs and the membrane potential required to elicit an AP, (**L**) number of APs elicited by injecting current in 20 pA intervals (median + range), and number of APs at 120pA in D2-MSNs from water or fentanyl abstinent mice (n=25 cells from 17 mice). See also Fig S2. Detailed statistics in Supplemental File 1.

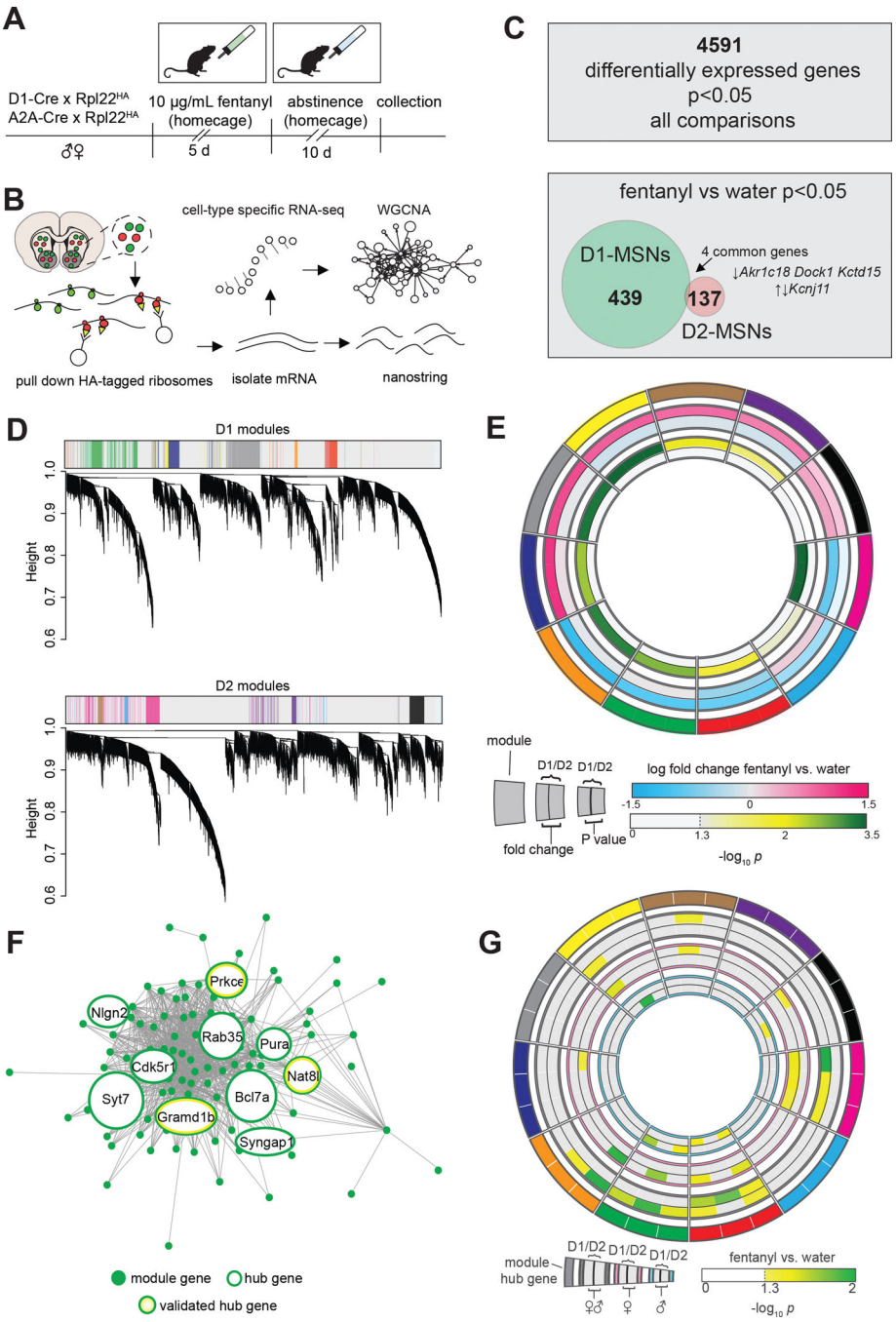

Figure 3. Translatome sequencing reveals MSN Subtype Specific Gene Co-expression networks in Fentanyl Abstinence

(**A**)Timeline for profiling MSN subtype translatomes in fentanyl abstinence. Male and female D1-and A2A-Cre mice were crossed with Cre-dependent ribosome tagged mice (Rpl22HA; RiboTag), then underwent homecage fentanyl drinking and abstinence (n=6 samples/sex/cell-type/drug, 4 mice pooled per sample). (**B**) HA-tagged ribosomes from D1- or D2-MSNs were immunoprecipitated and purified mRNA was used for Nanostring or to prepare cDNA libraries for RNAseq. Cell-type specific RNAseq data were analyzed by

Weighted Gene Co-expression Network Analysis (WGCNA). (**C**) Top: number of genes that exhibited a nominally significant effect ($p<0.05$) of fentanyl, sex, or cell type. Bottom: number of genes with nominally significant effect of fentanyl in D1- and D2-MSNs showing little overlap between subtypes. (**D**) Clustering dendrograms from analysis of the 4591 genes in D1- and D2-MSNs with WGCNA. Module colors are shown for modules pertaining to fentanyl abstinence, defined as differential module eigengene expression with $p<0.05$ effect of fentanyl abstinence. (**E**) Circos plot showing 11 selected WGCNA modules as arbitrary colors (outermost ring), ranked clockwise by overall fold change in D1-MSNs. Fold change in eigengene expression, and $-\log_{10}(P \text{ value})$ in D1- and D2-MSNs are shown internally. (**F**) Network structure of the green module. Hub genes are encircled in green, and the 3 hub genes selected for Nanostring are also encircled in yellow. Hub gene circle sizes are scaled based on the number of connections (**G**) Circos plot showing Nanostring analysis of 3 hub genes for each WGCNA module (outermost segments). Inner rings show fentanyl vs water differential expression scaled by $-\log_{10}(P \text{ value})$ with significant ($P<0.05$) differences featured in color. The outer comparison rings show data with males and females combined, while the pink and blue encircled rings show comparisons in females or males only. See also Fig S3, Table S1.

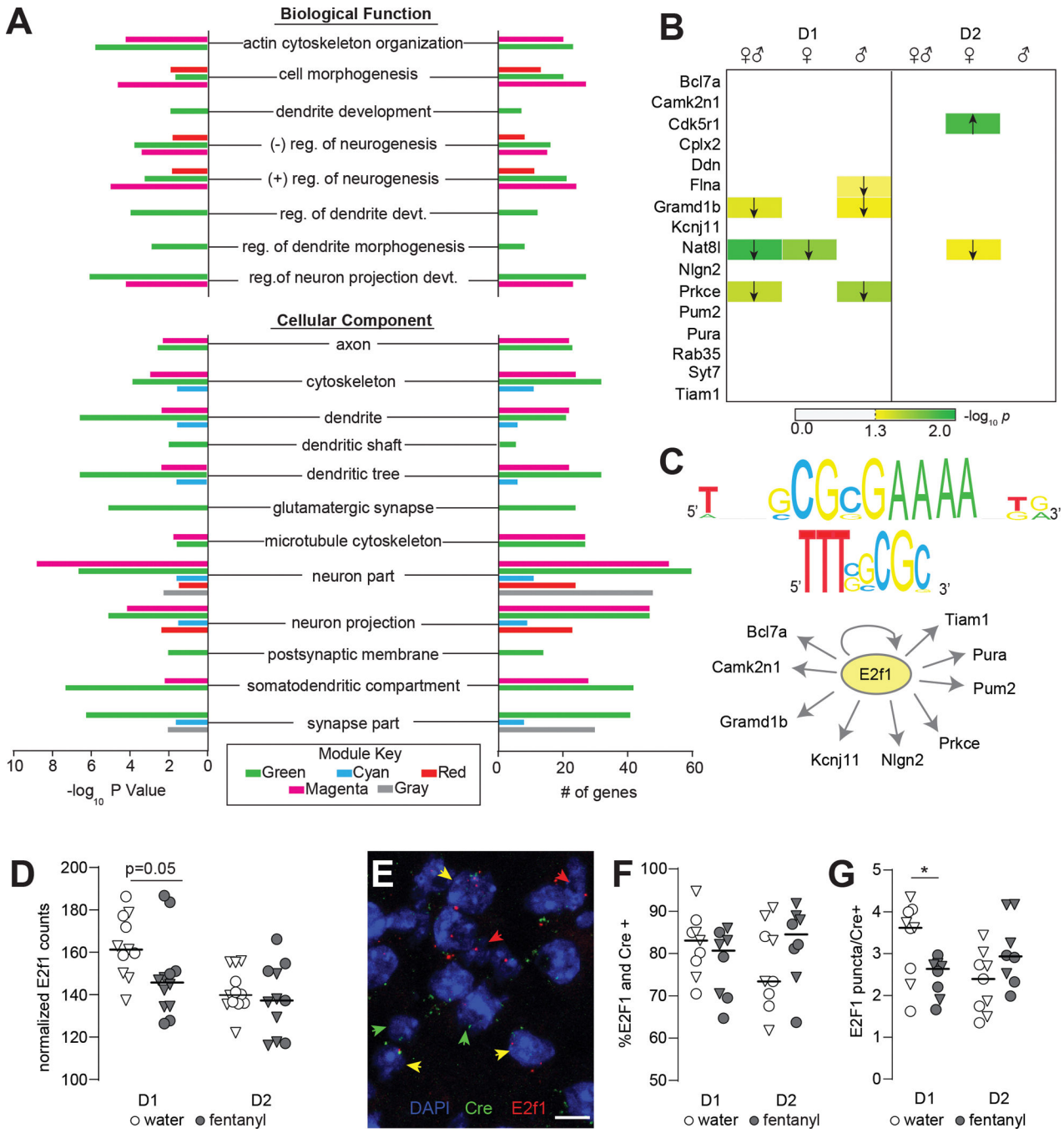

Figure 4. The D1-MSN specific Green Module contains downregulated dendritic morphology associated genes that are co-regulated by E2f1.

(**A**) Gene Ontology analysis showing enrichment of dendritic morphology related terms in green, cyan, red, magenta, and gray modules. (**B**) Nanostring validation of key green module genes in D1- and D2-MSNs showing differences in expression with sexes combined, and in males and females separately. Arrows denote direction of significant differences in expression between fentanyl and water. –$\log_{10}$(*P* value) is encoded in color. (**C**) Upstream regulator analysis with iRegulon indicates E2f1 is a predicted regulator of key green module

genes. Predicted binding motifs transfac_public-M00024 and yetfasco 627 shown above. (**D**) Nanostring counts showing decreased expression of E2f1 in D1-MSNs of fentanyl mice (n=6 samples/sex/cell-type/drug, 4 mice pooled per sample, p=0.05, unpaired t-test). Triangles denote males; lines indicate median. (**E**) Representative IMARIS reconstruction of fluorescence *in situ* hybridization for E2f1 in a D1-Cre mouse. DAPI stained nuclei are blue; red arrows denote E2f1 positive nuclei, green arrows denote Cre positive (D1 or D2), and yellow denote E2f1 and Cre positive nuclei. (Scale bar =10μm). (**F**) Percent E2f1 and Cre colocalized nuclei, and (**G**) number of E2f1 puncta per Cre positive nucleus in water and fentanyl abstinent mice. Each dot represents an individual mouse and is the sum of 3 separate images (~600 Cre+ nuclei counted per mouse; *, p=0.028,unpaired t-test). Triangles denote males; lines indicate median. See also Fig S3 and Supplemental File 2 and 3. Detailed statistics in Supplemental File 1.

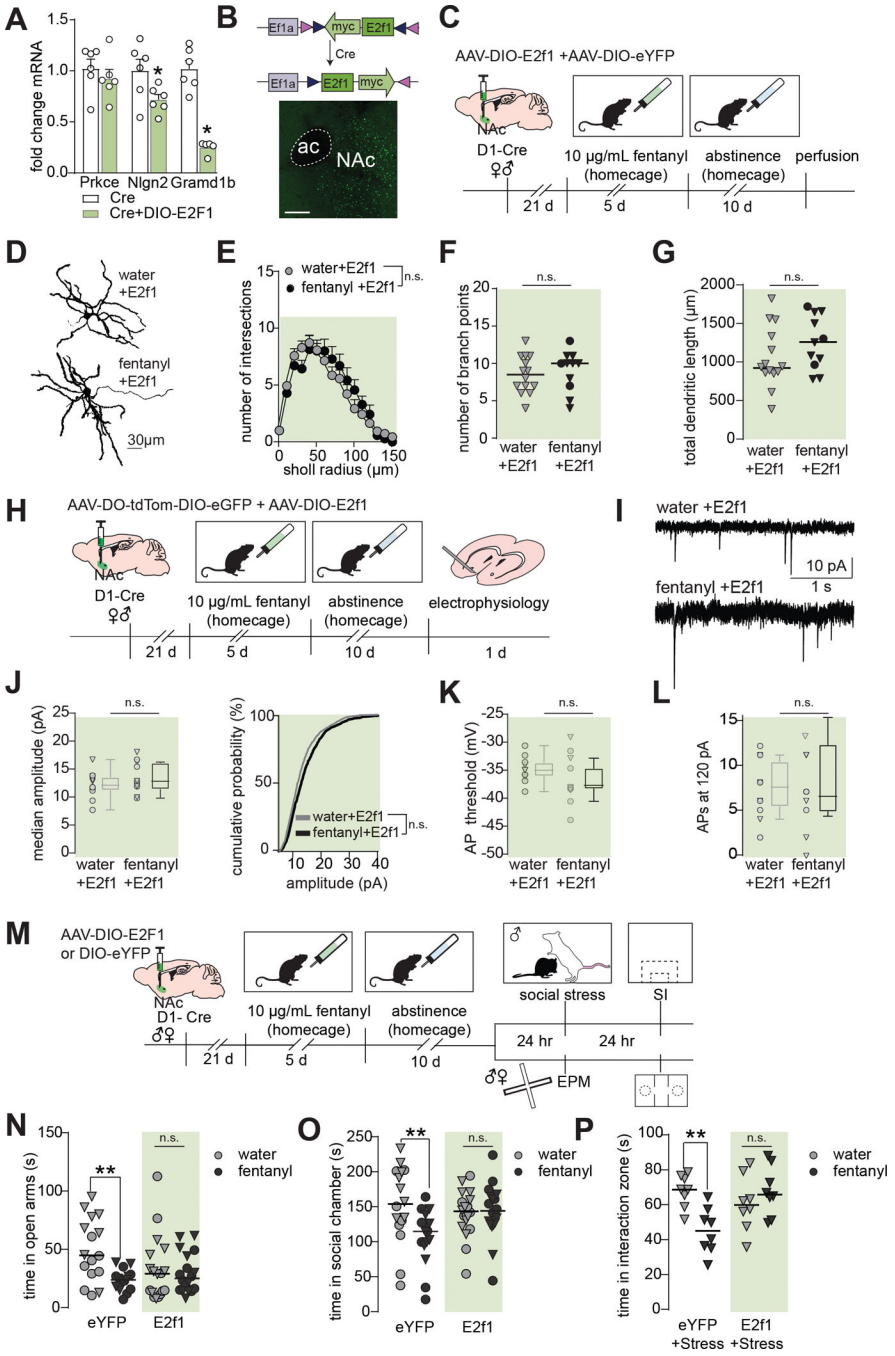

Figure 5. Increasing E2f1 in D1-MSNs is protective against abstinence-induced changes.

(A) Neuro2a cells were transfected with Cre and DIO-E2f1 or only Cre. qPCR analysis showing downregulation of E2f1 target genes Nlgn2 and Gramd1b (*, $p<0.05$, n=6 cultures per condition). Bars are mean ± sem (**B**) Top: Cre-mediated translocation of E2f1-myc-flag vector allowing for D1-MSN specific expression. Bottom: Representative photomicrograph showing AAV expression in the NAc. (**C**) Timeline for E2f1 morphology experiments. Male and female D1-Cre mice received AAV-DIO-E2f1 and a dilute AAV-DIO-eYFP to label D1-MSNs after fentanyl abstinence (**D**) Representative D1-MSNs from mice receiving

AAV-DIO-E2f1 prior to water or fentanyl abstinence. (**E**) Sholl analysis, (**F**) number of branch points, and (**G**) total dendritic lengths showing E2f1 prevents atrophy of D1-MSNs following fentanyl abstinence (E: mean±sem, Sidak's post-hoc after ANOVA, p>0.05; F-G:Nested t-tests, p's>0.05, n=28 cells from 9 mice; lines indicated median, triangles denote males). (**H**) Timeline for E2f1 electrophysiology experiments. Female and male D1-Cre mice received AAV-DO-tdTom-DIO-eGFP and AAV-DIO-E2f1 prior to undergoing fentanyl drinking and abstinence. Spontaneous excitatory postsynaptic currents (sEPSCs) were recorded from D1-MSNs while holding the membrane potential at −50 mV and analyzed by event detection. (**I**) Representative sEPSCs, (**J**) median sEPSC amplitude and cumulative probability in fentanyl+E2f1 and water+E2f1 mice (p=0.3, nested t-test; KS D=0.04 p=0.99). Individual data points represent individual neurons; triangles denote neurons from males. Box and whiskers plots show the median and range for data nested by mouse (n= 23 neurons from 15 total mice). (**K**) Membrane potential required to elicit an action potential (AP), and (**L**) the number of APs at 120 pA in fentanyl+E2f1 and water+E2f1 mice (p=0.23, p=0.75, repsectively). (**M**) Timeline for E2f1 behavioral experiments. Female and male D1-Cre mice received AAV-DIO-E2f1 or AAV-DIO-eYFP prior to undergoing fentanyl drinking and abstinence. A subset of male mice (top) was subjected to a one-day social stress paradigm, then assessed for stress-susceptibility 24hr later. The remaining mice underwent EPM and three-chamber social interaction testing. (**N**) Individual data points showing time water and fentanyl abstinent mice spent in the open arms of the EPM and (**O**) in the social chamber with a social target present (**, p's<0.008 eYFP-water vs eYFP-fentanyl, Sidak's post hoc). Lines indicate median, triangles denote males. (**P**). Individual data points showing time stressed water and fentanyl abstinent mice spent in the interaction zone with a novel target present. (**, p=0.003, eYFP-water vs eYFP-fentanyl, Sidak's post-hoc). See also Fig S4 and S5. Detailed statistics in Supplemental File 1.

Biol Psychiatry. Author manuscript; available in PMC 2024 March 15.

KEY RESOURCES TABLE

Resource Type	Specific Reagent or Resource	Source or Reference	Identifiers	Additional Information
Add additional rows as needed for each resource type	Include species and sex when applicable.	Include name of manufacturer, company, repository, individual, or research lab. Include PMID or DOI for references; use "this paper" if new.	Include catalog numbers, stock numbers, database IDs or accession numbers, and/or RRIDs. RRIDs are highly encouraged; search for RRIDs at https://scicrunch.org/resources.	Include any additional information or notes if necessary.
Antibody	anti-E2f1 for western	Abcam, Waltham, MA, USA	Cat#ab137415	
Antibody	anti-Prkce for western	Proteintech, Rosemont, IL, USA	Cat#20877-1-AP;RRID:AB_10697812	
Antibody	anti-Gramd1b for western	Proteintech, Rosemont, IL, USA	Cat#24905-1-AP;RRID:AB_2879791	
Antibody	anti-Nlgn2 for western	ProSci, Poway, CA, USA	Cat#7969	
Antibody	anti-GAPDH for western	Cell Signalling, Danvers, MA, USA	Cat#2118;RRID:AB_561053	
Antibody	Rabbit (DA1E) mAb IgG XP® Isotype Control (CUT&RUN)	Cell Signalling, Danvers, MA, USA	Cat#66362	
Antibody	Tri-Methyl-Histone H3 (Lys4) (C42D8) Rabbit mAb for Cut&Run	Cell Signalling, Danvers, MA, USA	Cat#9751;RRID:AB_2616028	
Antibody	anti-E2f1 for Cut&Run	Invitrogen,Waltham, MA *USA*	Cat#32-1400;RRID:AB_2533065	
Bacterial or Viral Strain	AAV5-Ef1a-DIO-eYFP	UNC Vector Core, Chapel Hill, NC, USA	RRID:Addgene_27056	
Bacterial or Viral Strain	AAV9-Ef1a-DO-TdTomato-DIO-EGFP	UMB Vector Core, Baltimore, MD, USA	RRID:Addgene_37120	
Bacterial or Viral Strain	AAV9-Ef1a-DIO-E2f1-myc-Flag	This manuscript, UMB Vector Core, Baltimore, MD, USA	N/A	
Biological Sample	mouse brain tissue	this manuscript	N/A	
Cell Line	Neuro2A cells	Sigma	Cat#89121404	
Chemical Compound or Drug	Fentanyl citrate	Cayman Chemical, Ann Arbor, MI, USA	Cat #22659	
Commercial Assay Or Kit	nCounter Master Kit--48 rxns NAA-AKIT-048	Nanostring, Seattle, WA, USA	Cat#100054	
Commercial Assay Or Kit		Advanced Cell Diagnostics,Newark, CA, USA	Cat#431971	
Commercial Assay Or Kit	RNAscope®			
Commercial Assay Or Kit	Probe - Mm-E2f1			
Commercial Assay Or Kit	RNAscope®	Advanced Cell Diagnostics,Newark, CA, USA	Cat#423321-C2	
Commercial Assay Or Kit	Probe - iCre-C2			
Commercial Assay Or Kit	RNAscope® Fluorescent Multiplex Reagent Kit	Advanced Cell Diagnostics, Newark, CA, USA	Cat#320850	

Resource Type	Specific Reagent or Resource	Source or Reference	Identifiers	Additional Information
Commercial Assay Or Kit	Cut & Run kit	Cell Signalling, Danvers, MA, USA	Cat#86652	
Commercial Assay Or Kit	nCounter GX CodeSet--48 rxns GXA-P1CS-048	Nanostring, Seattle, WA, USA	Cat#100021	
Deposited Data; Public Database	Differential expression and WGCNA	This paper	Mendeley Data, V1, doi: 10.17632/snpmrt8fj3.1	
Deposited Data; Public Database	RNA-seq data	This paper	GEO GSE209969	
Genetic Reagent				
Organism/Strain	RiboTag mice;B6J.129(Cg)-*Rpl22*$^{tm1.1Psam}$/SjJ	Bred at UMSOM	RRID:IMSR_JAX:029977	
Organism/Strain	A2A Cre mice;Tg(Adora2a-cre)KG139Gsat	Bred at UMSOM	Line KG139	
Organism/Strain	D1 Cre mice; Tg(Drd1-cre)FK150Gsat	Bred at UMSOM	Line FK150	
Organism/Strain	CD-1 mice, retired breeders	Charles River	RRID:IMSR_CRL:022	
Organism/Strain	C57Bl/6 mice	Bred at UMSOM	N/A	
Peptide, Recombinant Protein				
Recombinant DNA	Mouse E2f1-myc-Flag ORF clone	Origene	#MR206856	
Sequence-Based Reagent	Gramd1b Cut&Run primers	IDT DNA	Forward:TTAAGATGCGCCGGATGAAGA	
Sequence-Based Reagent			Reverse:GTCGCTGGAGGGCGTAATC	
Sequence-Based Reagent	Nlgn2 Cut&Run primers	IDT DNA	Forward:AATCAGCATGTGGCTCCTGG	
Sequence-Based Reagent			Reverse:GATCTCGTTGTTGAGCTCGC	
Sequence-Based Reagent	Prkce Cut&Run primers	IDT DNA	Forward:AGATCCGAGGAGCACAGACTC	
Sequence-Based Reagent			Reverse:ATAGAAAGTTTTGCCGGTTGGGG	
Sequence-Based Reagent	E2F1 primers	IDT DNA	Forward:CTCGACTCCTCGCAGATCG	
Sequence-Based Reagent			Reverse:GATCCAGCCTCCGTTTCACC	
Sequence-Based Reagent	Gramd1b primers	IDT DNA	Forward:CTGCCGTCCATTGAGATTACG	
Sequence-Based Reagent			Reverse:TCAGGAACCTGCTCGAATCAT	
Sequence-Based Reagent	Nlgn2 primers	IDT DNA	Forward:TGTCATGCTCAGCGCAGTAG	
Sequence-Based Reagent			Reverse:GGTTTCAAGCCTATGTGCAGAT	
Sequence-Based Reagent	Prkce primers	IDT DNA	Forward:GGGGTGTCATAGGAAAACAGG	
Sequence-Based Reagent			Reverse:GACGCTGAACCGTTGGGAG	

Resource Type	Specific Reagent or Resource	Source or Reference	Identifiers	Additional Information
Software; Algorithm	TopScan Lite	Cleversys, Reston, VA, USA	RRID:SCR_014494	
Software; Algorithm	Imaris 8.3	Bitplane, Oxford Intsruments	RRID:SCR_007370	
Software; Algorithm	nSolver	Nanostring	RRID:SCR_003420	
Software; Algorithm	pClamp	Axon Instruments	RRID:SCR_011323	
Software; Algorithm	MiniAnalysis	Synaptosoft	RRID:SCR_002184	
Software; Algorithm	TopHat		RRID:SCR_013035	
Software; Algorithm	HTSeq		RRID:SCR_005514	
Software; Algorithm	Weight Gene Co-Expression Network Analysis		RRID:SCR_003302	
Software; Algorithm	BiNGO plug-in for Cytoscape		RRID:SCR_005736	
Transfected Construct				
Other				